Annual Forcing of the Surface Radiation Balance Diurnal Cycle Measured from a High Tower near Boulder, Colorado

ELLSWORTH G. DUTTON

NOAA/ERL/ARL/GMCC, R/E/CG1, Boulder, Colorado

(Manuscript received 14 November 1989, in final form 25 April 1990)

ABSTRACT

The radiation balance consisting of upward and downward components of solar and thermal infrared broadband irradiances is continuously measured from the top of a 300-m tower situated on the Colorado high plains. The data are representative of a weighted areal average over a variety of surface and vegetation types within about a 1.5-km radius of the tower. Data from a three-year period, 1986–88, appears to be sufficient to define smooth annual cycles in monthly averages and 1-h resolution diurnal cycles in seasonal averages. It is found that even though infrared cycles are out of phase with cycles of corresponding solar components, the overall net radiation balance is in phase with surface solar forcing. The latter follows closely the extraterrestrial forcing but with some phase modifications by clouds and surface reflectance variations. The value of the correlation coefficient squared between the extraterrestrial radiation and the measured surface radiation balance quickly increases from 0.89–0.99 as averaging time increases from 1–90 days, respectively.

1. Introduction

A central question in global climate variability is the manner in which the earth's energy budgets are maintained. Energy budgets can be specified for portions of or the entire planet, atmosphere, or oceans, or across surfaces for which energy conservation can be ascertained. These budgets involve horizontal and vertical transfer of sensible and latent heat, mass, momentum, and radiation both into and out of a given system. [See North et al. (1981) for a review of energy balance modeling.] Of particular interest in climatology has been the energy balance at the earth's surface because of the great amount of energy exchange that occurs there. The surface radiation balance (SRB), that is, the net solar and infrared radiation at the surface, is a major component of the surface energy budget and is often determined separately because of its dominant magnitude and the relative difficulty in measuring the other components, the vertical fluxes of heat, moisture, and momentum. See Suttles and Ohring (1986) for additional discussion.

Although it has been possible to measure site-specific SRB from the ground for many decades, only recently has it been possible to achieve sufficient areal coverage and accuracy with satellites to obtain meaningful global coverage. However, ground-based observations still have an important role in providing higher absolute accuracy, better long-term stability, and higher temporal resolution than are normally possible from satellite. It is common to validate satellite estimates of surface radiation with ground-based observations (Tarpley 1979; Gautier 1982; Gautier and Katsaros 1984; Darnell et al. 1986; and others). An adequately observed SRB can also be used in connection with general circulation climate models (GCMs) for verification and analysis (Harshvardhan et al. 1989). General circulation climate models that accurately model the SRB gain credibility over those that do not.

This paper examines a three-year SRB record obtained at a single ground-based site, emphasizing monthly and seasonal variations in diurnal cycles relative to annual forcing. The surface-based observations are continuous, resolving temporal details of the SRB down to hourly averages. A similar study of a longer dataset, but limited to an unspecified surface in Hamburg, Germany, was given by Kasten (1977).

The near-surface radiation balance has been continuously measured for three years (1986–1988) from the top of the 300-m Boulder Atmospheric Observatory (BAO) tower. The tower is situated 20 km east of the base of the Rocky Mountains, in a dry plain agricultural area near Boulder, Colorado, and is operated by the National Oceanic and Atmospheric Administration (NOAA). The reflected and emitted irradiances from a representative variety of surface types and features are areally averaged using the data acquired at the 300 m height. The observed SRB is then potentially representative of a larger area with similar land surface. The atmospheric mass below 300 m AGL slightly modifies the measurements relative to true ground-level measurements, as discussed in section 2.

Corresponding author address: Ellsworth G. Dutton, Environmental Research Laboratories, (R/E/CG1), NOAA, 325 Broadway, Boulder, Colorado.

2. Data

On the BAO tower, downward and upward solar irradiances, or shortwave downward (SWD) and shortwave upward (SWU) irradiances, are separately measured with upward- and downward-facing Eppley pyranometers, which have a 2π-steradian field of view and are sensitive to 0.3–2.8 μm radiation. Likewise, longwave downward (LWD) and longwave upward (LWU) irradiances are measured with upward- and downward-facing Eppley pyrgeometers sensitive to $\approx$4–50 μm radiation in a 2π-steradian field of view. The upward-facing instruments are mounted at the highest level of the tower; only a very narrow (1.25-cm diameter) lightning rod extends above them. The downward-facing instruments are situated on the ends of booms extending three m out from the upper level of the tower. The downward-facing instruments view the surrounding rural area, which is quantified later in this section.

The radiometers' raw voltage and resistance measurements are acquired with a commercial data logger positioned at the top of the tower. The instruments are sampled every five seconds, but only hourly Universal Time Coordinated (UTC) averages are recorded. The hourly average raw data are routinely transferred to NOAA offices in Boulder over a telephone connection that also permits real-time interrogation of the data reduced to physical values in SI units for data quality control. An elevator provides access to the top of the tower for instrument inspection and maintenance.

The instruments are calibrated by the manufacturer, and checks and adjustments to the calibrations are made by the NOAA Radiation Facility in Boulder. Postprocessing involves applying the latest calibrations to the hourly average data, which are then plotted and screened for erroneous values. The data in this study were edited to remove data for times when the tower was enshrouded by clouds or the instruments were covered by snow, as determined by unreasonable albedos. The resulting values are believed to be accurate to better than the largest of $\pm$2% or $\pm$7 W m^{-2} for the SW and $\pm$5% for the LW, and to have a precision of better than $\pm$1% for both.

The interference resulting from the tower being in the field of view of the downward-facing pyranometer is corrected for by a permanently installed black plate near the instrument, which blocks the tower from the instrument. The black plate blocks 12% of the irradiance that would normally reach the sensor from an isotropic source and the instrument's calibration is adjusted accordingly. The plate actually blocks azimuth angles 330°N to 10° and biases the measurement accordingly relative to any bidirectional features in the reflected irradiance field. No similar correction is made in the downward-looking pyrgeometer since the tower is either emitting at or near the ground temperature or is reflecting LW radiation from the ground. The potential error in LWU due to the tower has not been further assessed.

The SRB results reported here should not vary significantly from a similar measurement limited to a single surface type in this area except for the magnitude of SWU. The relative contributions to SWU due to the different land surfaces within 1.1 km of the tower are given in Table 1. The results in Table 1 were determined on the basis of the surface area solid angle projected onto the downward-facing flat sensor at the tower top. The actual surface characteristics at any given time vary from year to year and from season to season. For reference, the accumulative contribution of the total land surface as a function of the distance from the tower is shown in Fig. 1. The representativeness of the BAO tower measurements relative to the larger surrounding region has not been assessed in detail. The principle advantage of the tower-top measurements is in viewing a variety of surface types, even though the exact contribution of each surface is not constantly monitored.

There is a small atmospheric contribution to an error in the tower-top measurements, relative to true surface measurements, because of the tower height. Calculations based on a model given by Cox (1973) and Griffith et al. (1980), and using Denver radiosonde data for the months of January and July 1987, show that the differences in LWU and LWD irradiance between the top of the BAO tower and ground level can be as large as 25 W m^{-2}, typical values being less than 10 W m^{-2}. However, usually the modeled LWU differences reverse sign from the 1200 UTC (0500 LST) sounding to the 0000 UTC (1700 LST) sounding, thereby tending to cancel in the daily mean, and go to zero sometime during midday and during the night. The modeled LWD tends to be greater at the surface than at the top by 2 W m^{-2} (1200 UTC) and 7 W m^{-2} (0000 UTC) in January and by 10 W m^{-2} in July for both daily soundings. Short-term measurements of SWD at ground level near the BAO tower and rough model calculations suggest only small solar irradiance

TABLE 1. Percentage of surface type projected onto the sensor measuring reflected shortwave upward (SWU) irradiance at BAO.

Description	Contribution (%)
Natural grass ($\approx$2% roads & buildings)	52
Rotation crops, unirrigated (bare soil or barley in alternate years; 5 fields)	19
Hay fields	8
Row crops, irrigated	7
Farm yards	5.5
Miscellaneous, roads, buildings	<1
Total	$\approx$93%*

* Remaining 7% is cultivated agricultural area beyond the monitored region, 1.1-km radius of tower.

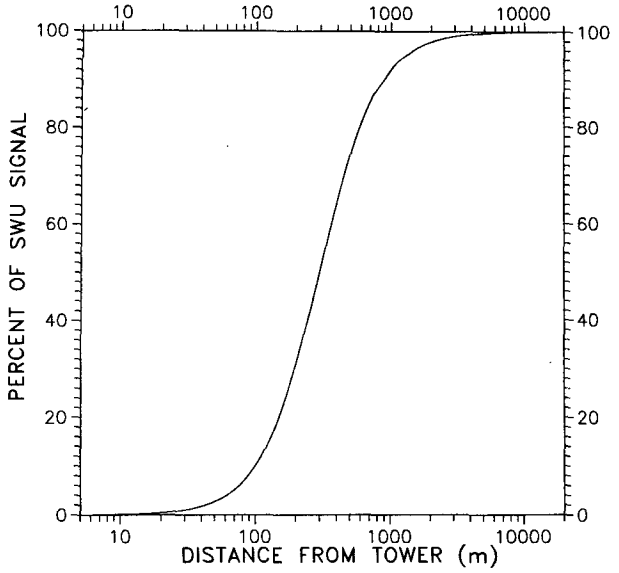

FIG. 1. Accumulative percentage of isotropic upwelling irradiance signal from a Lambertian surface, received by a flat-plate collector at the top of a 300-m tower, as the horizontal distance from the tower base increases.

differences, $\approx 1\%$, exist between the top and bottom of the tower. Any incoming solar loss in this layer due to Rayleigh and Mie scatterers would be backscattered into the SWU measured on the tower so that the solar flux divergence in the layer between the top of the tower and surface would be much smaller than any SWD loss. Therefore, the net shortwave (NSW) at the top would be nearly the same, well within 1%, as that at the ground level.

Vast amounts of surface radiation data have been collected around the world and have been accumulated and summarized by Budyko (1974), Sellers (1965), and Kessler (1985). A comparison between some BAO data and values applicable to the area are given in Table 2. The difference between BAO and Budyko data for December SRB can be accounted for depending on the extent of actual snow cover. An excellent presentation and discussion of diurnal and annual variation in the surface radiation balance from a number of locations is given by Kessler (1985).

3. Expected variations in SRB

Four sources of variability dominate the BAO SRB: diurnal cycles, annual cycles, cloud effects, and snow cover. Each of the four SRB components has different sources of variability.

SWD irradiance has the obvious diurnal and annual variations caused by the earth/sun geometry, but it also varies with atmospheric composition and cloudiness, the variations of which are not often well defined. Actual atmospheric conditions can potentially alter the phase and amplitude of the SWD diurnal and annual cycles relative to a diurnally and annually constant atmosphere. It is of interest to see how the other SRB components respond to modifications to the SWD cyclic forcing.

The SWU cycle instantaneously follows the SWD cycle except for changes in the surface albedo, which varies with vegetation and growing season, surface modification, moisture, snow cover, and incident angle of the sun. The areally averaged surface albedo at the base of the BAO tower can be slowly varying with season, diurnally variable with solar zenith angle, and irregularly variable with clouds and surface moisture, especially snow cover. The annual average energy-weighed albedo for 1986–88 for the BAO data was 0.216, but it varies from 0.15 to about 0.90 during the year.

Clear-sky LWD irradiance is a function of the vertically integrated atmospheric temperature, water vapor, ozone, carbon dioxide, and other trace constituents, but considerably more weight is given to the atmosphere nearest the instrument. LWD can be significantly affected by clouds, depending on the amount of moisture between the cloud and instrument, the air temperature, and the optical/physical composition of the cloud. The cloud base properties are particularly important if the clouds are thick because these clouds quickly become optically black within several hundred meters from their base (Paltridge and Platt 1976).

TABLE 2. Comparison between surface radiation data from the BAO tower and from other published sources.

Component	Surface radiation data: Time	Surface radiation data: BAO	Comparison reference
SRB	December	-23 W m^{-2}	+8 W m^{-2} (Budyko 1974)
SRB	Year	64 W m^{-2}	66 W m^{-2} (Budyko 1974)
SWD	January	109 W m^{-2}	104 W m^{-2} (Sellers 1965)
SWD	June	291 W m^{-2}	290 W m^{-2} (Sellers 1965)
SWD	December	97 W m^{-2}	86 W m^{-2} (Budyko 1974)
SWD	June	291 W m^{-2}	287 W m^{-2} (Budyko 1974)
SWD	Year	195 W m^{-2}	199 W m^{-2} (Budyko 1974)
Albedo	April	0.18	0.19–0.20 (Kung et al. 1964) (over eastern Colorado according to their plotted flight track)

Although LWU irradiance can be highly variable it has the fewest sources of variability, varying almost exclusively with the ground, or ground cover, effective radiative temperature. Variations due to changes in the emittance of the surface are not well known, and the ground is generally assumed to be black. Since the actual surface or "skin" temperature is not routinely measured at BAO, the actual surface emittance cannot be determined from the BAO data.

4. Forcing and response

Since there is usually a net gain of the solar radiation (shortwave) energy at the surface and a net loss of longwave radiation, it is convenient to consider the net shortwave (NSW = SWD − SWU) as forcing and the LW components as a response, although there are many complicated feedbacks. It is observed that the diurnal and annual cycles of LWD and LWU do lag the corresponding solar cycles. Of interest here is the manner in which the phase and amplitude of the component diurnal cycles in the SRB react to the annual cycle forcing of NSW.

As is seen in section 5b, there is a suggestion that the diurnal cycles of SWD and NSW at BAO are affected by a seasonal change in diurnal cloudiness. In this case the cloudiness could be considered forcing similar to that defined by Ramanathan et al. (1989). However, the idea of cloud forcing is complicated by clouds themselves responding to radiative forcing. This paper considers the forcing by the annual and diurnal solar extraterrestrial radiation (ETR) and the responses in the various annual and diurnal cycles in the SRB. The paper also considers the responses of the SRB diurnal cycles to the annual cycles in atmospheric variables such as temperature and clouds.

5. Analysis

a. Annual cycles

The annual cycle for each component of the BAO SRB was determined from three year monthly means of 24-h average irradiances (Fig. 2). The annual amplitudes are 194, 188, 105, 136, 32, and 167 W m^{-2} for SWD, NSW, LWD, LWU, net longwave (NLW), and net all-wave (i.e., SRB), respectively. SWU displays a bimodal cycle with a total annual range of 26 W m^{-2}. ETR, and subsequently NSW radiation, dominates the SRB, as evidenced by their phase relationships and the lack of strong cyclic forcing by either SWU or NLW. As might be expected, the LW components lag solar forcing by 1–2 months. NSW dominates the SRB annual cycle even though the LW components are larger in magnitude. LWU and LWD tend to cancel each other, to the extent that the NLW annual cycle is small compared with the NSW cycle. The annual cycle in air temperature at 300 m is also shown in Fig. 2. The LW cycles are in phase with the 300-m

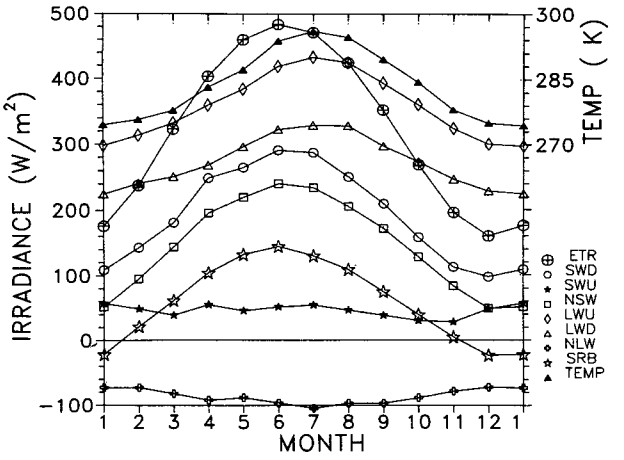

FIG. 2. Annual cycles of monthly mean BAO SRB components and 300 m air temperature. For clarity, individual solar components are shown.

temperature. Greater time resolution in this phase relationship analysis could be achieved by averaging over periods shorter than one month, but with only three years' data, this was not warranted. Following is a more detailed look at the SRB annual cycles.

The monthly total atmospheric transmission (TAT) can be defined as the ratio of SWD to the vertical component ETR. The monthly average TAT and ETR for 1986–88 BAO results are given in Table 3. Since there is no apparent annual cycle in TAT, it is suggested that to within the monthly resolution, sun/earth geometry dominates the annual phase of SWD. However, TAT is a strong function of solar zenith angle, as can be seen in clear-sky daily data. Therefore, with the considerable annual cycle in the monthly mean solar zenith angle at BAO, there should be an annual cycle in the monthly mean TAT given in Table 3. The absence of such a cycle indicates the presence of a compensating cycle in atmospheric transmission.

There are two opposing annual forcings in the SWU cycle: the annual cycle of ETR, and the albedo winter maximum due to snow cover. The SWU annual cycle is also influenced, to a lesser extent, by bidirectional effects and the annually changing daily mean solar zenith angle. The two opposing forcings tend to even out the yearly variability such that the SWD cycle, and hence the ETR, dominates the annual phase in NSW. Seasonal snowfall fluctuations and changing land use, primarily crop rotations, introduce the major potential for interannual variability in SWU.

Air and surface temperature, atmospheric moisture, and clouds control the LW cycles. A 20-yr climatology of Denver precipitable water monthly averages is exactly in phase with the temperature curve in Fig. 2. The TAT indicated the probable presence of an annual cycle in atmospheric solar transmission at BAO that is in phase with ETR. Since there is not a sufficient

TABLE 3. Monthly (1–12) average total atmospheric solar transmission (TAT = SWD/ETR) measured at the BAO tower, and calculated average vertical ETR (W m^{-2}) based on a solar constant of 1368 W m^{-2}, for 1986–1988.

	1	2	3	4	5	6	7	8	9	10	11	12
TAT	0.62	0.60	0.59	0.61	0.58	0.60	0.61	0.59	0.59	0.59	0.57	0.61
ETR	176	237	323	404	460	483	471	425	353	269	196	160

annual cycle in the other infrared radiators, CO_2 and O_3, to noticeably influence the mean annual variation of LWD, each of the LW annual cycles is driven by the ETR, with lags appropriate to the thermal inertia of the region. The NLW shows the greatest loss of energy in July, but the entire amplitude of the annual NLW is only 31 W m^{-2}, compared with 188 W m^{-2} for the NSW. Since the NLW annual cycle is relatively small and only $^1/_{12}$ cycle out of phase with NSW, there is negligible NLW effect on the annual phase of SRB. Therefore, the BAO SRB annual cycle, although influenced by many variables, is dominantly driven by (in phase with) ETR.

The strong correlation between the SRB and ETR is shown in Fig. 3. The value of the correlation coefficient squared between net SRB and ETR increases from 0.89–0.99 as the averaging time increases from 1–90 days, respectively, for the three year dataset at BAO. Therefore, a large percentage of the intraannual variance in the BAO SRB is accounted for by the geometric variations in the ETR. Stephens et al. (1981) showed that 95% of the annual planetary net radiation variance, as viewed from space, is also explained by ETR variation. Coincidently, Stephens et al.'s Fig. 13a also shows that the 95% value also applies specifically at the latitude and longitude of the BAO tower. The radiation budget variance accounted for by the ETR at the BAO location is apparently similar when viewed from space or the surface.

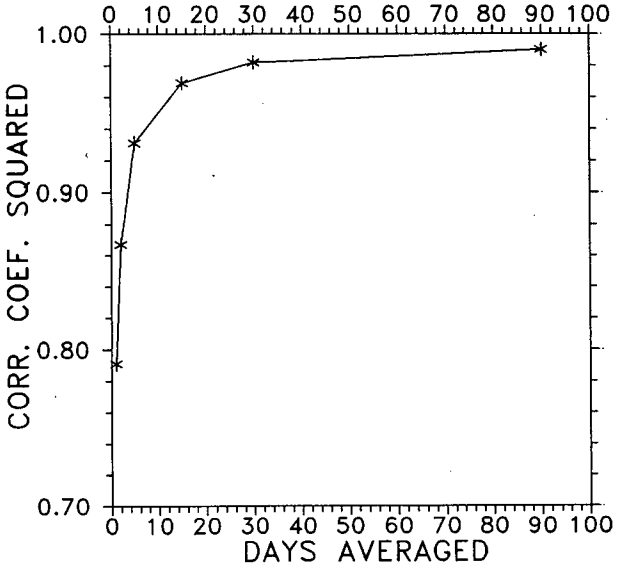

FIG. 3. Correlation between net SRB and ETR at the BAO tower plotted as a function of the averaging time for both components.

b. *Diurnal cycles*

It is not clear to what extent the SRB diurnal variations are climatologically significant. Randall et al. (1985) showed that the diurnal cycle is important in GCM simulations of global cloudiness, albedo, and annual precipitation over land. Average diurnal cycles of the BAO SRB were found by averaging the same hour of the day (LST) for an entire month or season and then averaging over the same month or season for the three years. This analysis would be more accurate if the data had been recorded with higher time resolution so that true solar noon had been better resolved; but only hourly resolution data are available without interpolation. The average diurnal cycle for each BAO SRB component is shown for each season in Fig. 4. The solar curves display the familiar bell shape, rising to a peak during midday. The LW cycles generally show a warming for about one-fourth of the day, beginning at or shortly after sunrise, rising to a peak after noon, and then cooling the remainder of the day and into the next. The phase and amplitude of the observed monthly average diurnal cycles can be used to investigate relationships between the various components and annual forcing.

If the diurnal cycle in NSW closely follows the diurnal ETR forcing, the peaks of SWD and NSW should coincide with the occurrence of true solar noon. The analysis is carried out in LST by identifying the hour in which true solar noon occurs and comparing that hour with the peak hour in the observed SWD or NSW. The results are indicated in Table 4. During the fall, winter, and spring months solar noon corresponds within a half hour to the maximum in the SWD and NSW. However, during the summer months the peak occurs before true solar noon, as seen in Fig. 4 as well as Table 4, suggesting that some other variable, most likely clouds, has modified the diurnal solar cycle at the surface.

There is a diurnal cycle in surface albedo (SWU/SWD), shown in Fig. 5, caused by solar zenith angle changes. The diurnal variation in albedo is mostly symmetric about solar noon in the spring, summer, and early fall, and therefore has little influence on the diurnal peak in NSW. The wintertime shift to an afternoon minimum in albedo does not have an obvious

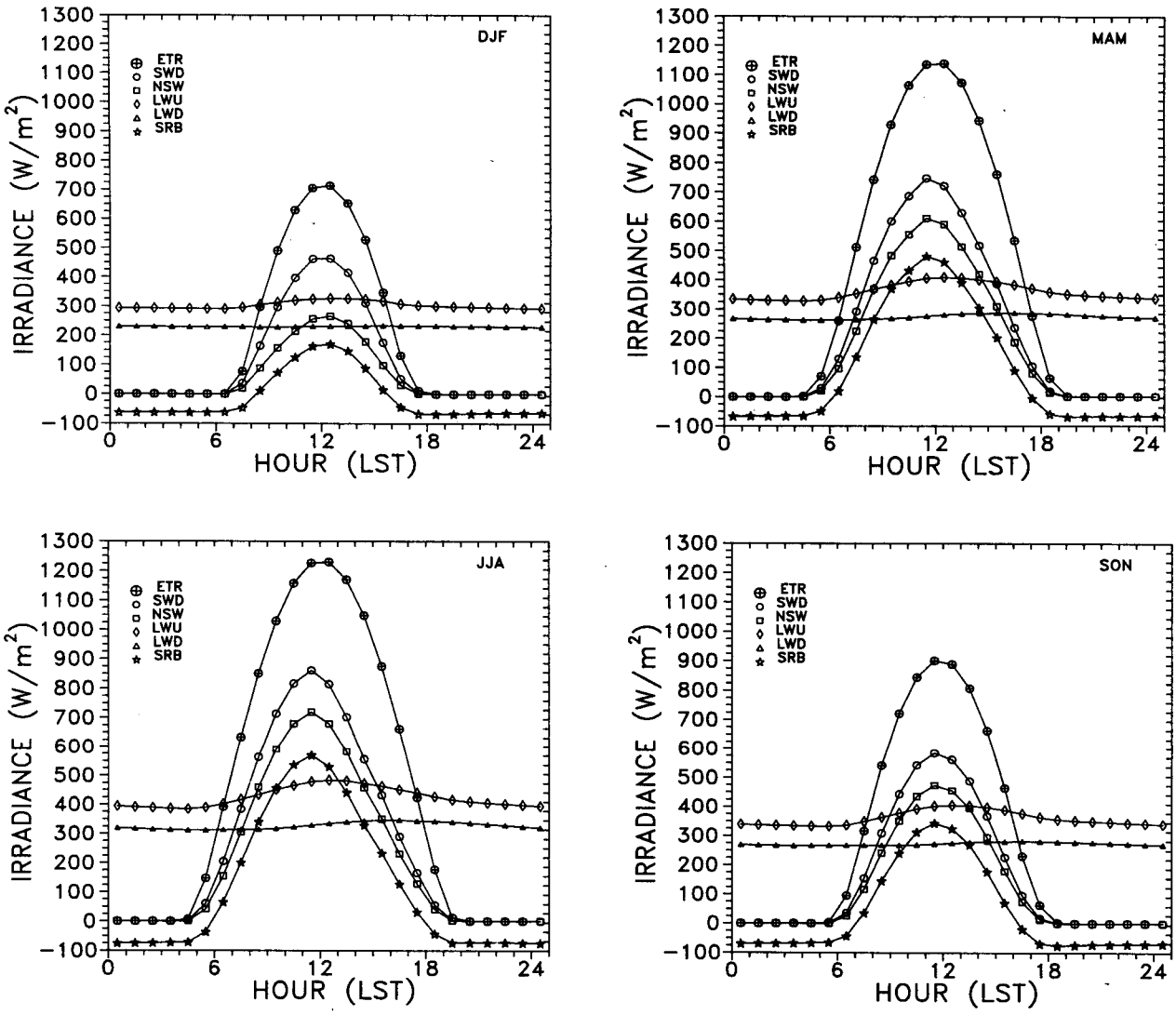

FIG. 4. Seasonal mean diurnal cycles of BAO SRB components for December, January, and February (DJF); March, April, and May (MAM); June, July, and August (JJA); and September, October, and November (SON).

TABLE 4. Hour (LST, 1–24) of peak in the average diurnal cycle for various components of the BAO SRB, based on hourly averages for 1986–1988. True solar noon (TSN) times are given for the 15th of the month.

	TSN	SWD	NSW	LWU	LWD	SRB
January	1209	13	13	13	16?	13
February	1214	13	13	13	18?	13
March	1209	12/13	12/13	13	15	12
April	1200	12	12	13	17	12
May	1156	12	12	13	17	12
June	1200	12	12	13	17	12
July	1206	12	12	13	17	12
August	1205	12	12	13	17	12
September	1155	12	12	13	17	12
October	1146	12	12	13	17	12
November	1145	12	12	13	18?	12
December	1155	12	12/13	13	?	12

effect on NSW except for about a half-hour shift toward afternoon in December (see Table 4). The wintertime shift in minimum diurnal albedo is probably caused by generally less snow on the ground later in the day and/or by possible overnight frost formation on the upward-facing pyranometer. The tendency for frost or dew formation on the sensors is unknown, although the top of the tower is commonly above the nighttime inversion and therefore condensation would not be expected in that situation.

Within the context of this study it is of interest to determine if modifications in the diurnal cycle of the NSW forcing could be traced to the LW components of the BAO SRB. We noted in Table 4 that the diurnal peaks in SWD, SWU, and SRB shift to earlier than true solar noon in June, July, and August. The LWU

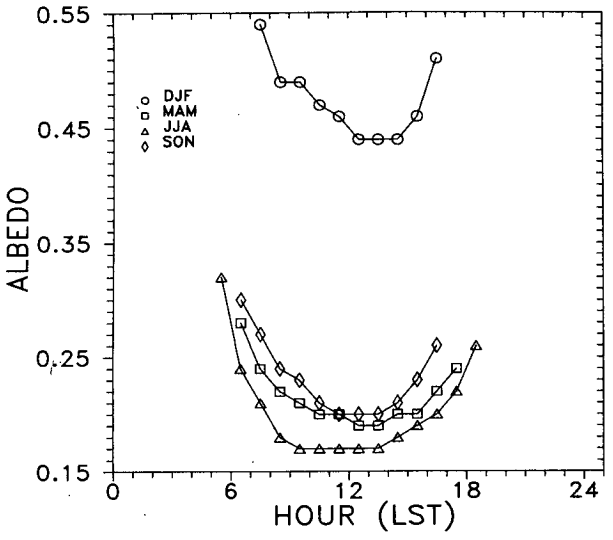

FIG. 5. Diurnal cycle of seasonal mean albedo at BAO.

peak is in the same hour as the NSW peak in January and February and lags into the next hour in April through November. A lag of less than an hour is indicated between NSW and LWU for December.

The diurnal lag between NSW and LWU peaks is noticeably less than the typical 2.5-h lag between diurnal solar heating and surface air temperature. This is to be expected, considering that the process for heating the actual surface (direct radiative absorption) operates faster than the processes for heating the air near the surface (convection and conduction, plus LW radiation). The diurnal cycle for LWU would then seem to be closely tied to that for NSW. Compared with LWD (Fig. 4), LWU has a much more well-defined response to solar forcing, as is shown by the change in slope at sunrise and sunset.

The diurnal cycle peak in LWD displays considerable variation over the year (Table 4), and becomes difficult to distinguish from November to February (at least in this dataset, which may be too short for better definition). When the LWD diurnal cycle is well defined, it lags the NSW cycle by a constant five hours from April through October. The lack of a wintertime diurnal cycle in LWD is probably due to reduced thermal convection and hence little diurnal heating above the top of the tower. This is indicated by the considerable diurnal surface heating seen in LWU and the lack of diurnal warming in LWD. The shape of the wintertime LWU diurnal cycle also suggests that heating near the ground is held there because the peak of the curve in winter is flatter than in summer (Fig. 4). The relative flatness of the winter LWD cycle compared with the summer cycle is confirmed by calculating the ratio of the numerical values adjoining the peak hour to the peak hour value. This phenomenon in the LWD is a function of the height above the ground at which the observations were made (see discussion in section 2). In the future, there will be an upward-facing LW sensor at the actual ground surface to determine LWD.

6. Annual forcing of the SRB diurnal cycles

Figure 6 shows the three year average time-of-year versus time-of-day contour plots of each of the four BAO SRB components as well as the ETR and SRB. Many of the features of the BAO SRB discussed in this paper are evident in Fig. 6. The contour plots are for data that were interpolated to obtain values at times other than those specifically recorded. The interpolated data could possibly be used to refine the analysis of diurnal cycle displacement (section 5b), but that has not been attempted here.

The annual variation in the BAO SRB diurnal cycles is clearly defined. The rate at which the diurnal cycles respond to the annual forcing is indicative of the inertia, or robustness, of the changing seasons. Figure 7 shows the annual variation in amplitude of the various SRB diurnal cycles. Note that the maximum and minimum diurnal amplitudes in the net SRB correspond to those of the SWD and NSW, which are in phase with the ETR maximum in June and minimum in December. Therefore, to within the one month resolution the net SRB diurnal cycle amplitude is in phase with the annual ETR forcing. Attempts to refine this analysis to higher time resolution, perhaps one week, were not made because of the shortness of the time series but could possibly be done with a few more years of data. Similarly, the LWD and LWU diurnal amplitudes follow, in phase, the corresponding LW annual cycles. There is, however, no reason to necessarily expect this correspondence between the annual and diurnal variations in LW.

The seasonal phase lag between ETR and average air temperature would cause the annual cycles of LWD and LWU to lag the annual solar forcing. However, it is not obvious why the amplitudes of the LW diurnal cycles would lag the solar diurnal forcing by a month, unless some factor other than the diurnal solar cycle is affecting the diurnal heating. One possible explanation is that since air temperatures are normally warmer in July than June, but since the slightly longer July nights permit greater nocturnal cooling, the diurnal ranges of LWD and LWU are amplified. Then, by August the diurnal solar forcing has decreased enough to again permit a decrease in the amplitude of the LW diurnal cycles, although the nights are even longer. However, once again there is little LW influence on the net SRB curve in Fig. 7 because of the small amplitude and in-phase character of the LW cycles.

7. Conclusions and discussion

The relationships between the phases and amplitudes of annual and diurnal cycles in the various broadband

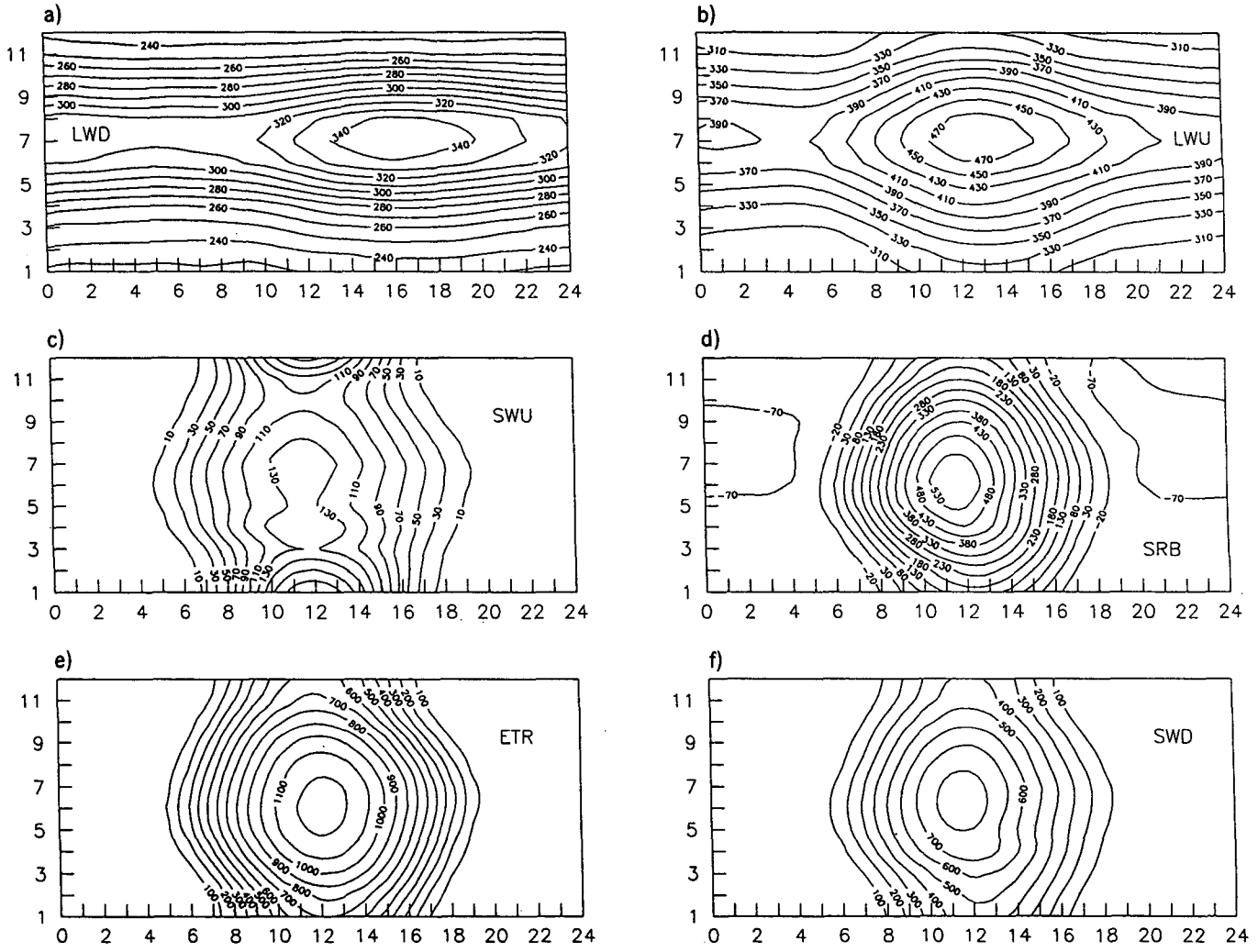

FIG. 6. Diurnal and annual variation of BAO SRB and individual components averaged over 1986–1988. Contours are equal irradiance in units of W m^{-2}. The month is plotted on the ordinate, and the hour of day is plotted on the absissa. The hour tics correspond to the actual LST time, and the month tics correspond to the midpoint of the month. (a) LWD, (b) LWU, (c) SWU, (d) SRB, (e) ETR, (f) SWD.

radiative components of a near-surface radiation balance were observed for a specific site. The observed relationships are of potential importance for climatological studies because they are broad band and are representative of an actual mixture of surface types. The results reported here would be difficult to observe from satellite or aircraft; the temporal detail of the surface-based observations is greater.

Annually, the surface SWD and NSW are in phase with the ETR. Because of the lack of a strong peak in either the diurnal or annual NLW, the net SRB closely follows NSW on time scales of a month or more. The magnitudes of the SWD and NSW diurnal cycles respond in phase to the annual ETR forcing, but the daily peaks are shifted, in summer by clouds and in winter (demonstrated only for December) by an afternoon minimum in albedo. The peak amplitudes of the LW diurnal cycles occur about a month later than the solar forcing peak.

Continuous BAO SRB data for three years appear to be sufficient to define smooth annual cycles and seasonal average diurnal variations. The monthly average diurnal cycles are less smooth in appearance, although well resolved for the most part. Weekly resolution of the diurnal cycles would be prohibitively degraded by cloud effects in this short data record. An increase in raw data resolution to better than one hour could be useful for studying diurnal cycle phase relationships in the SRB. A longer record would improve monthly resolution of annual variations, but then the phenomena under study would have to be constant for the longer time span.

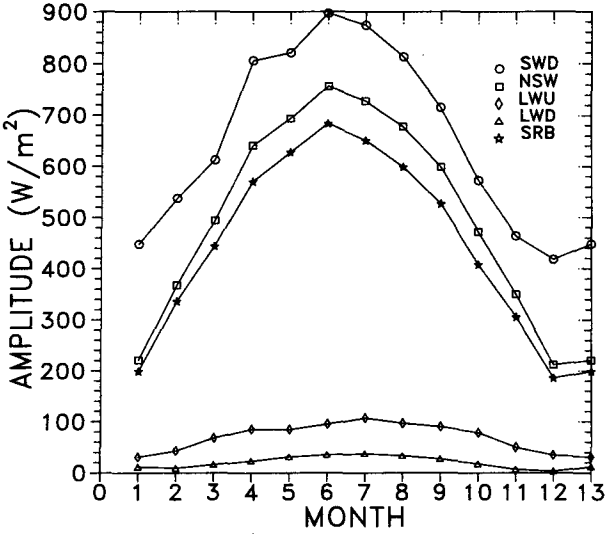

FIG. 7. Annual variation of the amplitude of various SRB diurnal cycles at BAO.

It is of interest to note that despite the highly variable hour-to-hour and day-to-day nature of the original BAO data (not shown), caused by short-term cloud variability, the depicted diurnal and annual cycles are relatively well determined and smoothly variable; the correlation between monthly average net SRB and ETR is equal to 0.98. This suggests that the net climatic effects of clouds on the SRB, on the time scale of 3 years, could be estimated by a simple adjustment to clear-sky model calculations. Likewise, future changes in this cloud adjustment based on future measurements could be used to monitor climatologically significant changes in cloudiness at the BAO measurement site.

Acknowledgments. I am grateful to Thomas McKee for suggesting this particular study, John DeLuisi for supporting the long-term measurement program, and Donald Nelson, Norbert Szczepczynski, and Daniel Wolfe for assisting with the measurements.

REFERENCES

Budyko, M. I., 1974: *Climate and Life.* Academic Press, 508 pp.

Cox, S. K., 1973: LW heating calculations with a water vapor pressure broadened continuum. *Quart. J. Roy. Meteor. Soc.*, **99,** 669–679.

Darnell, W. L., S. K. Gupta and W. F. Staylor, 1986: Downward longwave surface radiation from sun-synchronous satellite data: Validation of methodology. *J. Climate Appl. Meteor.*, **27,** 1012–1021.

Gautier, C., 1982: Mesoscale insolation variability derived from satellite data. *J. Appl. Meteor.*, **21,** 201–206.

——, and K. Katsaros, 1984: Insolation during STREX. Part 1: Comparisons between surface measurements and satellite estimates. *J. Geophys. Res.*, **89,** 11 779–11 788.

Griffith K, S. K. Cox and R. Knollenburg, 1980: LW radiative properties of tropical cirrus clouds inferred for aircraft measurement. *J. Atmos. Sci.*, **37,** 1077–1087.

Harshvardhan, D. A. Randall, T. G. Cossetti and D. A. Dazlich, 1989: Earth radiation budget and cloudiness simulations with a general circulation model. *J. Atmos. Sci.*, **46,** 1922–1942.

Kasten, F., 1977: Daily and yearly time variation of solar and terrestrial radiation fluxes as deduced from many years records at Hamburg. *Solar Energy,* **19,** 589–593.

Kessler, A., 1985: *World Survey of Climatology, Vol. 1A,* Elsevier Press, 224 pp.

Kung, E. C., R. A. Bryson and D. H. Lenschow, 1964: Study of a continental surface albedo on the basis of flight measurements and structure of the earth's surface cover over North America. *Mon. Wea. Rev.*, **22,** 543–564.

North, G. R., R. F. Calahan and J. A. Coakley, 1981: Energy balance climate models. *Rev. Geophys. Space Phys.*, **19,** 91–121.

Paltridge, G. W., and C. M. R. Platt, 1976: *Radiative Processes in Meteorology and Climatology.* Elsevier Press, 198 pp.

Ramanathan, V., R. D. Cess, E. F. Harrison, P. Minnis, B. R. Barkstrom, E. Ahmad and D. Hartmann, 1989: Cloud-radiative forcing and climate: Results from the earth radiation budget experiment. *Science,* **243,** 57–63.

Randall, D. A., J. A. Ables and T. G. Corsetti, 1985: Seasonal simulations of the planetary boundary-layer stratocumulus clouds with a general circulation model. *J. Atmos. Sci.*, **42,** 641–676.

Sellers, W. D., 1965: *Physical Climatology.* University of Chicago Press, 272 pp.

Stephens, G. L., G. G. Campbell and T. H. Vonder Haar, 1981: Earth radiation budgets. *J. Geophys. Res.*, **86,** 9739–9760.

Suttles, J. T., and G. Ohring, 1986: Surface radiation budget for climate applications. NASA Ref. Pub. 1169, 132 pp.

Tarpley, S. D., 1979: Estimating incident solar radiation at the surface from geostationary satellite data. *J. Appl. Meteor.*, **18,** 1172–1181.